Single-molecule resolution of interfacial fibrinogen behavior: Effects of oligomer populations and surface chemistry

Mark Kastantin, Blake B. Langdon, Erin L. Chang, and Daniel K. Schwartz*

Department of Chemical and Biological Engineering, University of Colorado, Boulder, Colorado 80309

*To whom correspondence should be addressed

daniel.schwartz@colorado.edu

Supporting Information

Analytical Ultracentrifugation

Materials and Methods

A Beckman XL-A analytical ultracentrifuge equipped with UV adsorption optics was used to make measurements at a wavelength of 230 nm approximately every 4 minutes. A 1 cm long cell was placed 6.3 cm from the center of rotation. A rotor speed of 30,000 rpm was used at 25°C. Alexa Fluor ® 488 labeled human fibrinogen samples with a concentration of 1.0 μM in PBS were dialyzed overnight at 4°C against PBS to remove residual salts from the labeling and lyophilization process. Velocity sedimentation was carried out overnight in PBS at two initial fibrinogen concentrations of 40 and 74 nM.

The fibrinogen concentration distribution was measured as a function of time and the distance from the center of rotation. After background subtraction, this concentration distribution was numerically fit to the Lamm equation describing the evolution of the concentration distribution evolution of a species with a given diffusion coefficient and sedimentation coefficient (s) using the Sedfit program.[1] From this fit the sedimentation coefficient distribution, $c(s)$ was determined. The frictional coefficient was fit to the data using the Sedfit program and an initial guess calculated using the Svedberg equation.[2, 3]

Results

Analytical ultracentrifugation was used to determine the relative fractions of fibrinogen monomer and oligomer in solution. The sedimentation coefficient distribution can be seen in Figure S1. The peak at lower sedimentation coefficient for 40 and 74 nM injection concentrations corresponds to fibrinogen monomer populations with average sedimentation coefficients of 8.8 ± 0.6 S and 8.6 ± 0.4 S, respectively. The peak at higher sedimentation coefficient corresponds to objects with average sedimentation coefficients of 14 ± 1.5 S and 13 ± 1.1 S for the 40 and 74 nM injection concentrations, respectively. By integrating the area under each peak in Figure S1, the fraction of the monomer in solution was found to be 0.94 ± 0.02 where the error represents the standard deviation between measurements taken at the two concentrations.

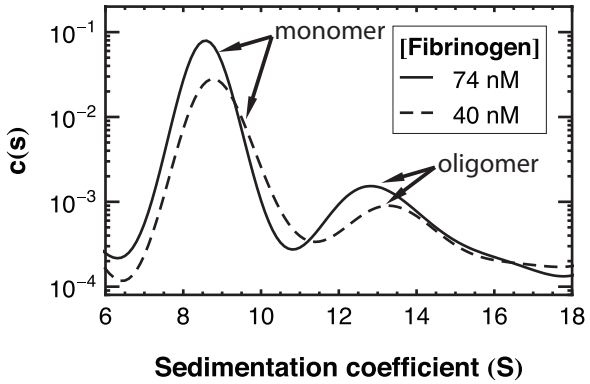

Figure S1. The sedimentation coefficient distribution of fluorescently labeled human fibrinogen at 40 and 74 nM loading concentrations calculated from analytical ultracentrifugation experiments.

Size-Exclusion Chromatography

Materials and methods

Size-Exclusion Chromatography (SEC) was also used to investigate fibrinogen monomer and aggregate populations in solution. Analysis was performed with a Beckman Coulter Systems Gold HPLC system, associated UV 166 detector (set at 230 nm) and a Wyatt Dawn EOS multi-angle detector positioned at a scattering angle of 90°. A TSK-Gel G3000SW column (Tosoh Biosciences) at room temperature was used in fibrinogen studies with a mobile phase of PBS. Studies were carried out at a flow rate of 1.0 mL/min for 30 minutes with a 100 μL injection volume for a 0.5 μM solution of Alexa Fluor ® 488 labeled human fibrinogen, kept at 4°C for 8h prior to injection. ASTRA software was used for peak integration of UV absorption data.

Results

SEC was used as an orthogonal technique to AUC in order to determine the relative fractions of fibrinogen monomer and oligomer in solution. In Figure S2, light-scattering data indicates two distinct fibrinogen populations. The first peak corresponds to the shoulder in the major peak of UV absorbance and is indicative of fibrinogen aggregates. The major peak in the absorbance

trace of Figure S2 represents the fibrinogen monomer population and accounts for a weight fraction of 0.95 ± 0.01 where the error represents the standard deviation of multiple trials. Monomer fractions were determined by integration of the UV absorbance signal over the time interval corresponding to the peak in the scattering signal. These values are consistent with those calculated in AUC experiments.

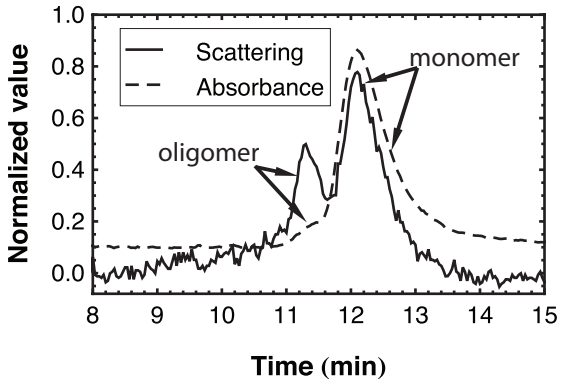

Figure S2. SEC results showing absorbance and light-scattering traces of fluorescently labeled human fibrinogen at room temperature in PBS.

Additional tables and figures

Diffusion coefficients for populations A-D

The numerical values for diffusion data presented in Figures 3 and 5 are given in Tables S1 - S3, along with uncertainties representing 95% confidence in the last significant figure given.

Table S1. Parameters used to fit equation (2) to the experimental cumulative squared-displacement distributions on the FS surface.

Population	**Intensity units**	**Residence time (s)**	x_1 **D_1 (μm²/s)**	x_2 **D_2 (μm²/s)**	$\overline{D}$ **(μm²/s)**
A	0.51-0.77	4	1 0.0197(2)		0.0197(2)
B	1.9-2.2	4-6	0.13(2) 0.028(3)	0.87(2) 0.0084(2)	0.0109(7)
C	2.8-3.0	10-14	0.36(1) 0.0118(2)	0.64(1) 0.00340(5)	0.0064(1)
D	3.6-4.1	50-120	0.168(5) 0.0100(2)	0.832(5) 0.00238(2)	0.0037(1)

Table S2. Parameters used to fit equation (2) to the experimental cumulative squared-displacement distributions on the TMS surface.

Population	**Intensity units**	**Residence time (s)**	x_1 D_1 (μm²/s)	x_2 D_2 (μm²/s)	x_3 D_3 (μm²/s)	$\overline{D}$ (μm²/s)
A	0.49-0.74	4	1 0.0284(2)			0.0284(2)
B	1.9-2.1	4-6	0.85(2) 0.0198(2)	0.15(2) 0.0044(6)		0.0175(4)
C	2.8-3.1	10-14	0.55(1) 0.0166(2)	0.45(1) 0.0029(1)		0.0104(2)
C'	2.8-3.1	40-120	0.12(5) 0.020(3)	0.62(3) 0.006(1)	0.26(5) 0.0016(2)	0.007(1)
D	3.6-4.0	40-120	0.07(1) 0.019(2)	0.84(1) 0.0032(6)	0.09(1) 0.00015(4)	0.0042(2)
D'	3.6-4.0	10-14	0.41(2) 0.0155(6)	0.59(1) 0.0025(1)		0.0078(4)

Table S3. Parameters used to fit equation (2) to the experimental cumulative squared-displacement distributions on the PEG(5000) surface.

Population	**Intensity units**	**Residence time (s)**	x_1 D_1 (μm²/s)	x_2 D_2 (μm²/s)	x_3 D_3 (μm²/s)	$\overline{D}$ (μm²/s)
A	0.50-0.75	4	1 0.0138(1)			0.0138(1)
B	1.9-2.1	8-12	0.32(1) 0.0132(2)	0.68(1) 0.00419(4)		0.0071(2)
C	2.7-3.0	20-26	0.01(1) 0.03(2)	0.33(5) 0.006(1)	0.66(6) 0.0027(1)	0.0041(6)
D	3.8-4.0	70-200	0.017(4) 0.0261(4)	0.246(2) 0.00456(3)	0.737(3) 0.00163(1)	0.0028(1)

Cumulative distributions for first, middle, last, and all steps in a trajectory

The cumulative squared-displacement distributions used to generate Figure 6 are shown in Figure S3 for fibrinogen on fused silica. The tail of the distribution for "middle" and "all" steps decays more quickly than that for "first" and "last" steps in a trajectory, indicating that fast diffusion is more likely to follow adsorption and precede desorption.

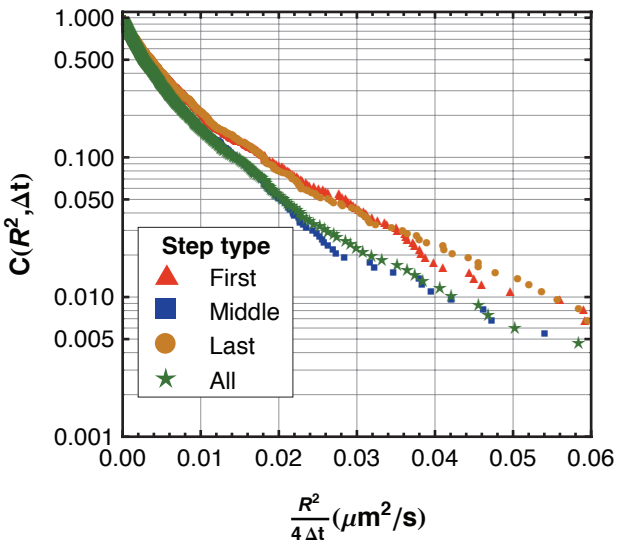

Figure S3. The cumulative squared-displacement distributions are shown for different positions in trajectories observed on a fused silica surface. These distributions were used to produce the values given in Figure 6.

Atypical protein populations

Table S2 shows two populations that have not been previously mentioned, C' and D' on TMS surfaces. These populations have the intensity selection criteria of populations C and D but the residence time selection criteria from neighboring populations. This method of transposing residence time selection criteria with different populations was done for all populations on all surfaces and typically did not change the observed diffusive behavior since molecules of the same intensity have the same aggregation number regardless of characteristic residence time. In the cases of C' and D', however, diffusive behavior was observed that was drastically different than populations C and D. That is to say that the x_j and D_j for population C' are closer to those of population D than C. Similarly, values for population D' are closer to those of population C than D. This suggests that while the primed populations have the same aggregation state as their unprimed counterparts (based on intensity data), they have different three-dimensional arrangements of fibrinogen monomers that cause surface interactions atypical of their aggregation number.

Interestingly, these atypical populations were observed only on the hydrophobic TMS surface. This suggests that fibrinogen-TMS interactions may exist at specific local contact points where the protein or aggregate has exposed hydrophobic regions. Consequently, the precise geometric arrangement of fibrinogen monomers within the aggregate can give rise to surface interactions of varying strength while maintaining the same aggregation number. Put another way, one arrangement of monomers may expose more hydrophobic patches to the exterior of the aggregate than another and the type of surface may or may not have any influence over the preferred arrangement. In contrast, the FS and PEG(5000) surfaces may interact very weakly with fibrinogen, but over the entire contact area of the protein. The combined effect of all these weak interactions is therefore insensitive to subtle differences in the arrangement of monomers in an aggregate. The above-mentioned difference between hydrophobic and hydrophilic surfaces is reminiscent of the multiple observed energy barriers for fibrinogen desorption from hydrophobic colloidal probes by Xu and Siedlecki whereas only a single barrier was observed using hydrophilic probes.[4] However, neither the present work nor that of Xu and Siedlecki provides concrete evidence of the mechanism leading to this difference and further efforts directed at understanding this phenomenon should be undertaken.

Representative images and surface uniformity

Figure S4 shows representative images from TMS surfaces at several different times. Diffraction-limited spots are randomly distributed throughout the images and no other surface features are visible indicating uniformity of the underlying surface. Surface uniformity was quantified by mapping the mean residence time as a function of position. A movie was captured

on a representative TMS-coated surface with a 0.2 ms frame exposure time for 10 minutes in order to observe more molecules in a given area and increase the spatial resolution of the map. The resulting map is shown in Figure S5 with bins that are 1.45 μm on a side. Mean residence times are mostly under 2 seconds while some mean values approach 5 seconds. Some heterogeneity is to be expected for random adsorption of a heterogeneous population onto a uniform surface. More importantly, the areas with higher mean residence times are not different than the mean residence time over the entire surface (1.6 s) with any reasonable statistical significance. This provides evidence that the surface is devoid of micron-scale defects that might support anomalously strong fibrinogen adsorption. Similar results are observed on representative PEG and FS surfaces.

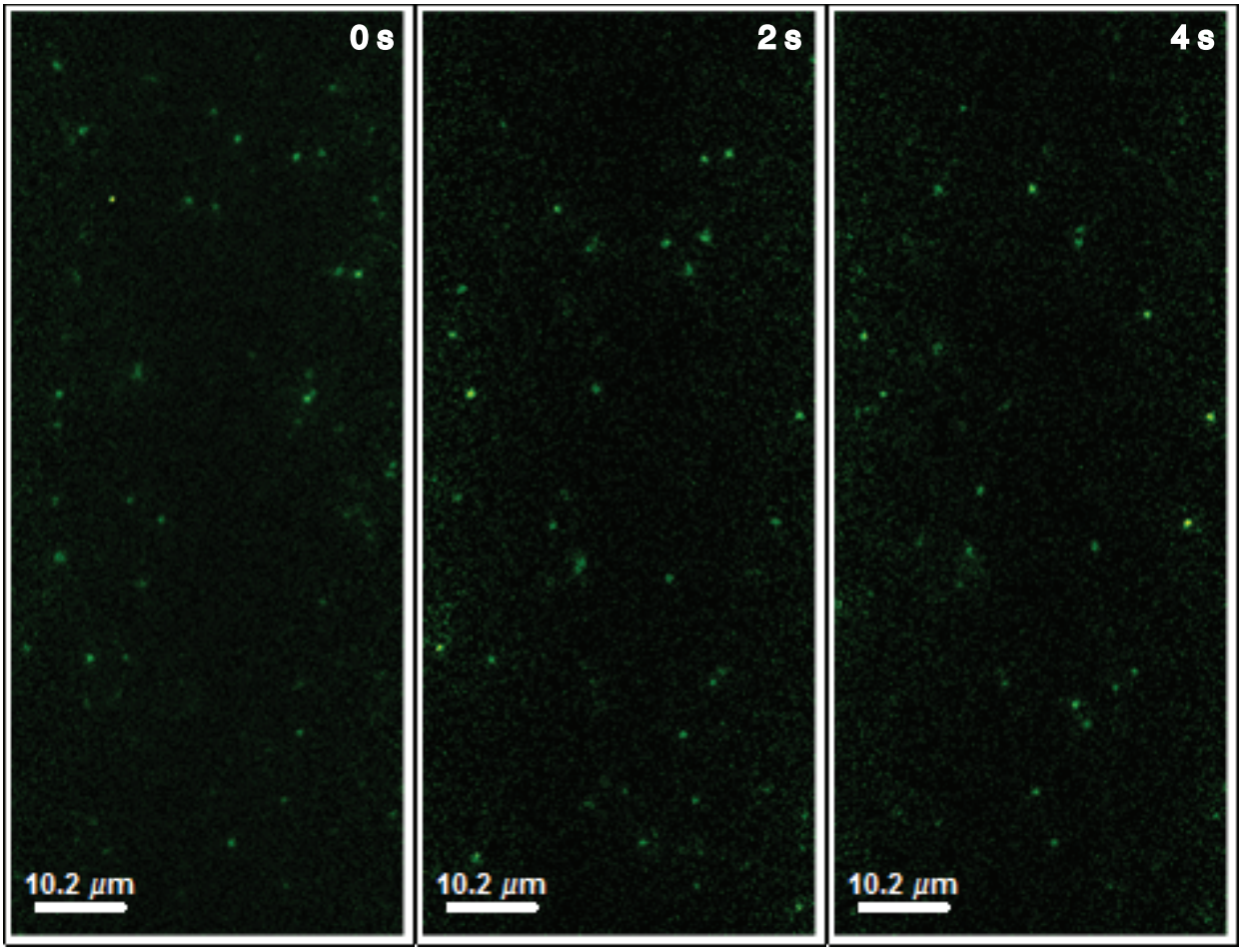

Figure S4. A sample sequence of images from fibrinogen on a TMS-coated substrate is shown. Bright diffraction-limited spots are the main features in each image with background noise appearing as faint, smaller spots. Image convolution with a disk matrix increases recognition of diffraction-limited spots over background noise.

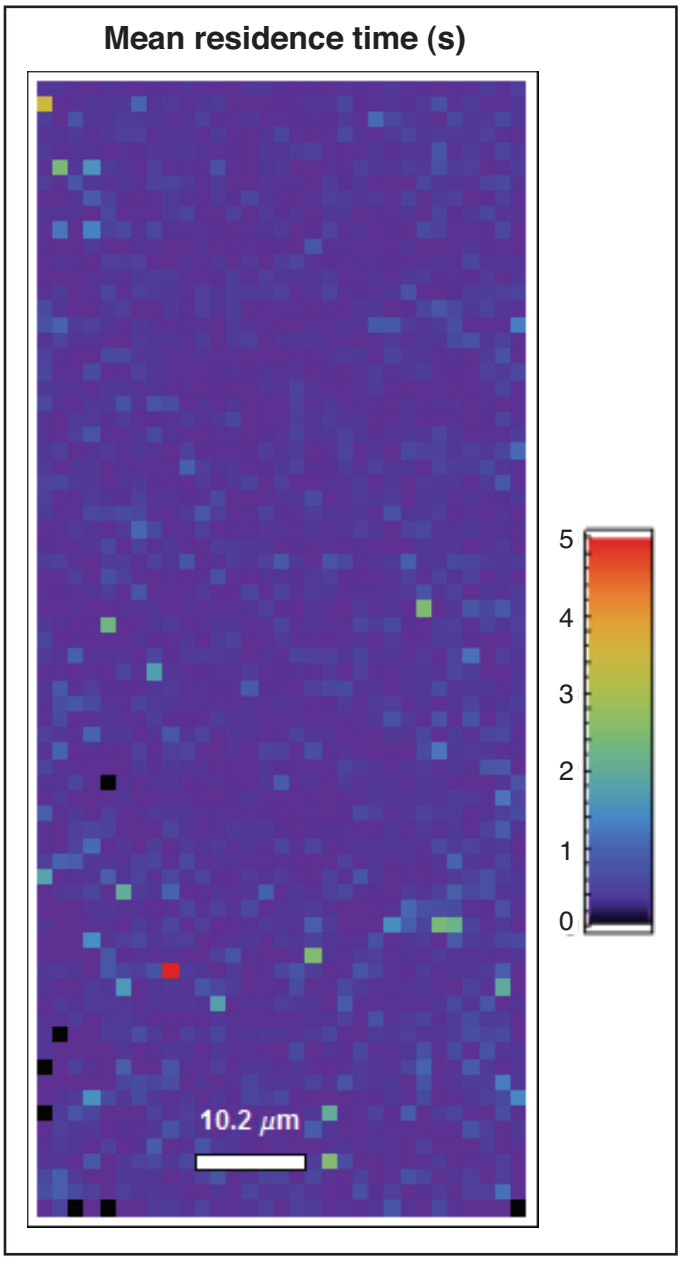

Figure S5. The mean residence time of all objects that adsorbed in a given area is shown as a function of position on a TMS-coated surface. Each bin is 1.45 μm on a side. This surface mapping demonstrates that micron-scale surface heterogeneities that could lead to anomalous protein-surface attraction are not present. Most mean values are less than 2 seconds but all mean values are not statistically different than the surface-averaged mean residence time of 1.6 seconds. Black represents areas in which no objects were observed to adsorb.

References

1. Schuck, P., *Biophysical Journal* **2000,** *78* (3), 1606-1619.
2. Johnson, P.; Mihalyi, E., *Biochimica Et Biophysica Acta* **1965,** *102* (2), 476-486.
3. Robert, C. H., *Biophysical Journal* **1995,** *69* (3), 840-848.
4. Xu, L. C.; Siedlecki, C. A., *Langmuir* **2009,** *25* (6), 3675-3681.